Available online at www.sciencedirect.com
SCIENCE DIRECT®
Journal of Sound and Vibration 283 (2005) 433–448
JOURNAL OF SOUND AND VIBRATION
www.elsevier.com/locate/jsvi

Particle impact damping: effect of mass ratio, material, and shape

Kun S. Marhadi, Vikram K. Kinra*

Department of Aerospace Engineering, Center for Mechanics of Composites, Mail Stop 3141, Texas A&M University, College Station, TX 77843-3141, USA

Received 22 December 2003; accepted 24 April 2004

Abstract

Particle impact damping (PID) is measured for a cantilevered beam with a particle-filled enclosure attached to its free end. PID due to different particle materials is measured: lead spheres, steel spheres, glass spheres, tungsten carbide pellets, lead dust, steel dust, and sand.

1. Introduction

Particle impact damping (PID) is a method to increase structural damping by inserting particles in an enclosure attached to a vibrating structure. The particles absorb kinetic energy of the structure and convert it into heat through inelastic collisions between the particles and the enclosure, and amongst the particles themselves. The unique aspect of PID is that high damping is achieved by converting kinetic energy of the structure to heat as opposed to the more traditional methods of damping where the elastic strain energy stored in the structure is converted to heat.

Perhaps one of the earliest applications of impact damping for controlling the vibrations of cutting tools, milling radial drills, gear hobbing machines, and other machinery was described by Harris and Crede [1]. Using the principles outlined by Erlikh [2], Ryzhkov [3] reported a design of an impact damper for metal cutting tools. The damper was found to substantially reduce some of

*Corresponding author. Tel.: +1-979-845-1667; fax: +1-979-845-6051.
E-mail address: kinra@aero.tamu.edu (V.K. Kinra).

0022-460X/$ - see front matter © 2004 Elsevier Ltd. All rights reserved.
doi:10.1016/j.jsv.2004.04.013

Nomenclature

c	reduced damping coefficient of the beam
d	clearance of the enclosure
g	acceleration of gravity = 9.81 m/s^2
m	mass of the particles
m_e	end mass of the beam
m_{encl}	mass of the enclosure
A	cross-sectional area of the beam
K	reduced stiffness of the beam
L	length of the beam
M	primary mass
N	number of particles
R	effective coefficient of restitution
T	maximum kinetic energy during a cycle
ΔT	kinetic energy dissipated during a cycle
U	displacement amplitude of the primary mass
V	velocity amplitude of the primary mass
v_p	velocity of the particle
Δ	dimensionless clearance
Γ	dimensionless acceleration amplitude
Γ_{cr}	critical dimensionless acceleration amplitude
Ψ	specific damping capacity
Ψ_m	mass normalized damping
μ	mass ratio
ω	undamped circular natural frequency
ρ	mass density of the beam
Ψ_b	specific damping capacity of beam material
ζ	damping ratio

the detrimental effects of vibration such as premature and uneven loss of sharpness of the cutting edge and bad surface quality of the machined component. A systematic analytical/experimental study of the damping due to a single impact damper in free and forced vibration in the horizontal plane was reported by Bapat and Sankar [4]. They studied the effect of mass ratio, coefficient of restitution, gap size (or clearance), and frequency.

Saluena et al. [5] have studied analytically the dissipative properties of granular materials using particle dynamic method. They showed how the analysis of energy-loss rate displays different damping regimes in the amplitude–frequency plane of the excitation force. Tianning et al. [6] performed numerical modeling of particle damping with discrete element method. They showed that under different vibration and particle system parameters, the collision and friction mechanism might play different or equivalent roles in energy dissipation.

Some experimental studies have also been conducted to measure particle impact damping. Papalou and Masri [7] studied the behavior of particle impact dampers in a horizontally vibrating single-degree-of-freedom (SDOF) system under random base excitation. Using tungsten powder, they studied the influence of mass ratio, container dimensions, and excitation levels. They provided optimum design of particle damper based upon reduction in system response. Cempel and Lotz [8] used a simplified energy approach to measure the influence of various particle-packing configurations on the damping loss factor of a SDOF system under horizontal forced vibration. Popplewell and Semercigil [9] conducted experiments to study the performance of a plastic "bean bag" filled with lead shot in reducing vibration. They observed that a plastic bean bag not only exhibited a greater damping effectiveness but also "softer" impacts than a single lead slug of equal mass. Panossian [10,11] conducted a study of non-obstructive particle damping in the modal analysis of structures. This method consists of drilling small diameter cavities at appropriate locations in a structure and partially or fully filling the holes with particles of different materials and sizes. Significant decrease in structural vibrations was

observed even when the holes were completely filled with particles and subjected to a pressure as high as 240 atm.

More recently, Friend and Kinra [12] conducted an experimental investigation of particle impact damping in the context of free decay of a cantilever beam with the enclosure attached to its free end, and vibrating in the vertical plane. They studied the effects of vibration amplitude and particle fill ratio (or clearance) on damping. PID was observed to be highly nonlinear, i.e. amplitude dependent. A very high value of maximum specific damping capacity (~50%) was observed in the experiment. An elementary analytical model was also constructed to capture the essential physics of PID. A satisfactory agreement between the theory and experiment was observed. All the experimental results were obtained with only one mass ratio, one material (lead powder), one particle size (230 μm), and three values of clearance. PID in a horizontal plane was studied experimentally and numerically using a discrete element method by Saeki [13]. Their model was able to predict the experiments with a "reasonable accuracy".

One can measure damping in either steady-state time-harmonic motion or in transient motion. The goal of the work by Friend and Kinra [12] was to develop a theoretical/experimental model that can be used to suppress *transient vibration* of a structure; hence, the choice of a cantilevered beam undergoing free decay vibrations as the platform for their experimental study. In the present work, following Friend and Kinra [12], all measurements of particle impact damping were carried out using a cantilevered beam undergoing free decay vibrations. The primary objective of this work is to report additional PID measurements obtained with particles of different materials (lead spheres, steel spheres, glass spheres, sand, steel dust, lead dust, and tungsten carbide pellets), particle sizes (0.2–3 mm), clearances, and number of particles.

2. Theoretical analysis

In the following, a summary of the theory developed by Friend and Kinra [12] is presented. The reader is referred to Ref. [12] for additional details. The theory begins with the idealization of the beam as a standard Euler–Bernoulli beam vibrating in its fundamental mode, and the enclosure as a point mass (m_{encl}) attached to the tip of the beam. The continuous beam is then reduced to an equivalent SDOF; see Fig. 1. The reduced mass of the beam, referred to the free end ($x = L$), is found to be 0.24 of the actual mass of the beam (i.e., $0.24\rho AL$; where ρ is the mass density, A is area of cross-section, and L is the length of the beam). Therefore, the primary mass of the equivalent SDOF system is $M = 0.24\rho AL + m_{\text{encl}}$. Similarly, the reduced stiffness (K) of the vibrating beam was found to be $3.01EI/L^3$ which is almost equal to the static stiffness of the beam loaded at its tip ($3EI/L^3$).

Let ω be the circular frequency of the fundamental mode, and ψ_b be the *intrinsic material damping* of the beam material. The reduced damping coefficient of the beam is given by

$$c = \frac{\psi_b}{2\pi}\sqrt{KM}. \tag{1}$$

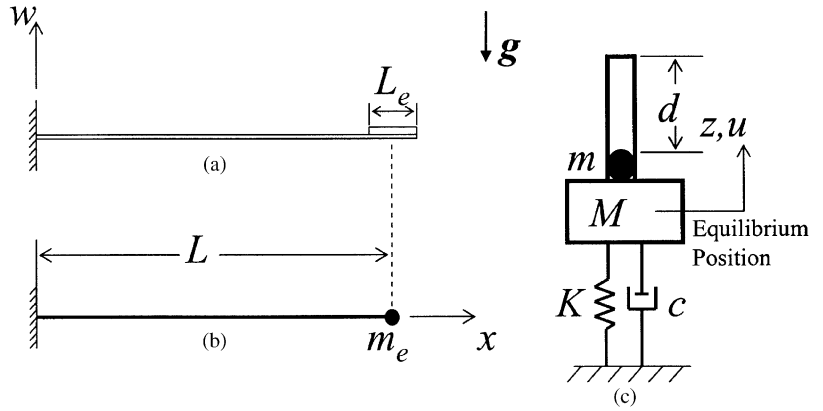

Fig. 1. (a) A schematic of the beam and enclosure (drawn to scale). (b) A model of the beam with end mass, m_e. (c) The equivalent single-degree-of-freedom (SDOF) system. The displacement, u, of the mass, M, is measured from its equilibrium position with the particle mass, m, resting on the bottom of the enclosure. The origin of the coordinate z is also located at the equilibrium position of M. The vector $\mathbf{g}$ is the acceleration due to gravity.

Then, the damping ratio, $\zeta = c/c_{cr} = c/(2\sqrt{KM}) = \psi_b/4\pi$. Since in Ref. [12] the exact mode shape of the beam is used to compute M and K, the undamped natural frequency of the equivalent SDOF system, $\sqrt{K/M}$, is *exactly* equal to the undamped natural frequency of the first mode of the beam, ω; the same is true for the damped natural frequency. Moreover, for the beam used in this study, the damped natural frequency may be approximated by its undamped natural frequency, i.e., $\omega_d \approx \omega$.

In most vibration problems the mass of the beam remains constant. Therefore, the static deflection due to the weight of the beam also remains constant and is neglected. The problem at hand is a little bit more complicated: there are times when the particles move in contact with the beam, and at other times they move separately from the beam. To keep the model simple, first it is assumed that all particles move as a lumped mass, m, i.e., the relative motion between the particles is neglected. It follows then that the end mass, m_e, is a two-valued function. Moreover, the static deflection due to gravity is no longer a constant. Therefore, the static deflection must be taken into account in the analysis of the problem; see Ref. [12] for the derivation of the equations. With this observation, the analogy between the continuous beam (Fig. 1(b)) and its equivalent discrete SDOF system (Fig. 1(c)) is complete.

Specific damping capacity (Ψ) is defined as the kinetic energy converted into heat during one cycle (ΔT) normalized with respect to the maximum kinetic energy of the structure during the cycle (T),

$$\Psi = \Delta T/T, \tag{2}$$

where T is given by

$$T = \tfrac{1}{2}MV^2. \tag{3}$$

The energy dissipated during the ith cycle is calculated using

$$\Delta T_i = T_i - T_{i+1}. \tag{4}$$

Since the experiment cannot determine whether or not the particles are in contact with the enclosure at any given instant, it is assumed that the particles are in contact with the enclosure at velocity peaks. Then, m_{encl} (and therefore M) includes the mass of the particles, m, and the energy dissipated can be expressed as

$$\Delta T_i = \tfrac{1}{2}M(V_i^2 - V_{i+1}^2). \tag{5}$$

Substituting Eqs. (5) and (3) into Eq. (2), damping during the ith cycle is expressed as

$$\Psi_i = \frac{V_i^2 - V_{i+1}^2}{V_i^2}. \tag{6}$$

Friend and Kinra [12] introduced a parameter R (effective coefficient of restitution) that is a measure of the total energy dissipated during one cycle due to all possible mechanisms of energy dissipation (for example, inelastic collisions and frictional sliding amongst the particles, and between the particles and the enclosure). Defining v_p^- (v_p^+) and v_2^- (v_2^+) to be, respectively, the velocity of the "particle" and the primary mass before (after) an impact, R was defined as

$$R = -\frac{(v_p^+ - v_2^+)}{(v_p^- - v_2^-)}, \quad 0 \leqslant R \leqslant 1. \tag{7}$$

The energy dissipated during an impact is given by

$$\Delta T = \tfrac{1}{2}(1 - R^2)\frac{m}{1+\mu}(v_p^- - v_2^-)^2, \tag{8}$$

where $\mu = m/M$ is the ratio of the mass of the particles to the primary mass. R is estimated by minimizing the difference between the theory and the experiment using the method of least squares. There are several parameters that affect energy dissipation during an impact,

$$\Delta T = f(m, d, g, M, \omega, U; R), \tag{9}$$

where g is the gravitational constant, ω is the fundamental frequency (in rad/s) of the beam, d is the clearance (i.e. the distance between the top of the bed of particles at rest and the ceiling of the enclosure), and U is the vibration amplitude. The semicolon separating R is used to emphasize that R is obtained by curve-fitting experimental data to the model. In dimensionless parameters, Eq. (9) becomes

$$\Psi = f(\mu, \Delta, \Gamma; R), \tag{10}$$

where $\Delta \equiv d\omega^2/g =$ dimensionless clearance, and $\Gamma \equiv U\omega^2/g =$ dimensionless amplitude.

3. Experimental procedures

A schematic of the experimental setup is shown in Fig. 2. A particle enclosure is attached to a cantilevered beam made of 4140 steel (Young's modulus, $E = 207\,\text{GPa}$ and density $= 7.84 \times 10^3\,\text{kg/m}^3$). The clearance, d, can be varied by adjusting the ceiling of the enclosure using

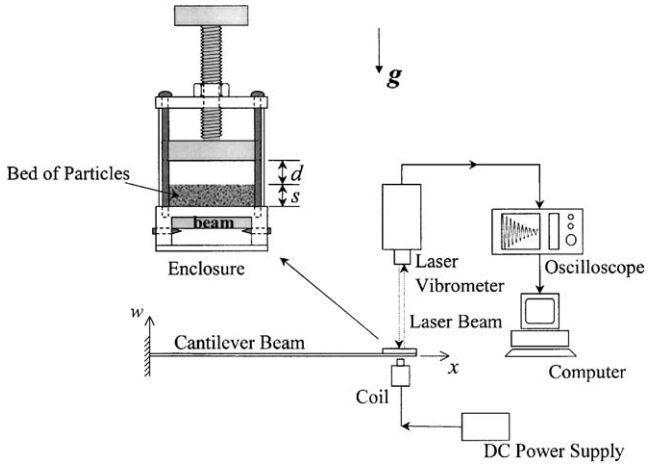

Fig. 2. A schematic of the experimental setup. Detail of the enclosure with an adjustable clearance.

a threaded screw. The mass of the empty enclosure is 67.1 g and its interior dimensions are: diameter = 19.1 mm and maximum height = 25.4 mm. The cantilever beam dimensions are: length = 306.6 mm, width = 19.16 mm, and height = 3.16 mm. The mass of the beam is 145.5 g. The natural frequency of the fundamental mode of the beam with the enclosure attached was measured to be 16.7 Hz. The equivalent mass of the SDOF system is 102 g. The intrinsic material damping of the beam was found to be about 1%, which is small compared to PID.

A coil connected to a DC power supply is used to provide a constant magnetic force to a steel plate mounted to the bottom of the enclosure. The vertical position of the coil is adjusted to provide an initial displacement, U_0. At time $t = 0$, the current to the coil is switched off, and the beam is allowed to decay freely.

A OFV300 Polytec laser vibrometer is used to measure velocity of the enclosure. Data acquisition is triggered at $t = 0$, and the decaying waveform is collected with a Yokogawa DL708 Digital Processing Oscilloscope (DPO). The digitizing rate is set at 2000 points/s. For a nominal frequency of 16 Hz observed in this study, this translates to 125 points/cycle.

The particles tested followed by their diameters in parentheses are as follows: lead spheres (1.2 mm), steel spheres (1.17 mm), glass spheres (0.5, 1.12, and 3 mm), irregular tungsten carbide pellets (equivalent diameter 0.5 mm), sand (equivalent diameter 0.2 mm), steel dust (equivalent diameter 0.5 mm), and lead dust (equivalent diameter 0.2 mm). These materials are chosen for the great diversity in their density: glass (2.5×10^3 kg/m^3), steel (7.84×10^3 kg/m^3), lead (11.3×10^3 kg/m^3), and tungsten carbide (13×10^3 kg/m^3). Most of the experiments are conducted with a particle mass of 6.5 g, which corresponds to a mass ratio, $\mu = 0.06$. Tests are conducted with the dimensionless clearance, $\Delta = 1.13, 2.26, 3.36, 4.52, 5.25, 5.65$, or 7.91, and $1 \leqslant \Gamma \leqslant 10$. Damping for each cycle, Ψ_i, is determined using Eq. (6). For each clearance, tests are repeated eight times with different initial amplitudes. The results are presented as a compilation of these repeated tests. The damping due to particles alone is then determined by subtracting the intrinsic material damping of the beam from the total damping.

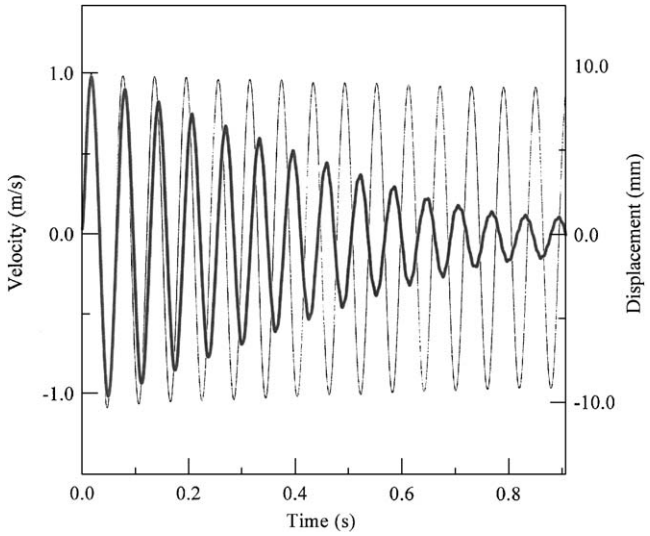

Fig. 3. A comparison of typical experimental velocity waveforms with and without particles. 1.2 mm lead spheres, $\mu = 0.1$ and $\Delta = 5.65$. Frequency = 16 Hz. ___, Without particles; ═══, with particles.

4. Experimental results

Typical decay curves for the beam with and without particles are shown in Fig. 3 (1.2 mm lead spheres with $\mu = 0.1$ and $\Delta = 5.65$). Clearly, PID causes a significant decrease in the amplitude within the first few cycles. Corresponding to these data, the energy dissipated per cycle is presented in Fig. 4 as a function of maximum velocity at the beginning of each cycle, along with the maximum kinetic energy. Through a casual examination of Fig. 3 (bold line) it would be tempting to fit a straight line through the peaks. This was done by Bapat and Sankar [4]. This implies a tacit assumption that Ψ decreases *linearly* with time. For the limited data reported in Ref. [4] this appears to have been a good assumption. However, in this work we do not make this or any other assumption about the dependence of damping on any of the independent variables. Instead, by computing the damping on a cycle-by-cycle basis, we explore the dependence of Ψ on the independent variables. As may be seen in the following figures, Ψ is highly *nonlinear*.

4.1. The effect of mass ratio

In Ref. [12], all measurements were made for a fixed value of $\mu = 0.12$. We begin by studying the effect of μ on $\Psi(\Gamma)$ while keeping Δ fixed (at $\Delta = 5.65$) and using 1.2 mm lead spheres. In Fig. 5(a), Ψ is plotted against Γ for three values of $\mu = 0.02, 0.04$, and 0.1. As expected, $\Psi = 0$ for $\Gamma < 1$: for acceleration less than 1 g, the particles never leave the floor [12]. The maximum PID is roughly 10%, 20%, and 40%, respectively. The significance of Γ_{cr} has been explained in detail in Ref. [12]. For $\Gamma < \Gamma_{cr}$, the particles begin to fall down before they hit the ceiling; there are no impacts with the ceiling. For $\Gamma < \Gamma_{cr}$, the first impact of the particles is with the ceiling; this

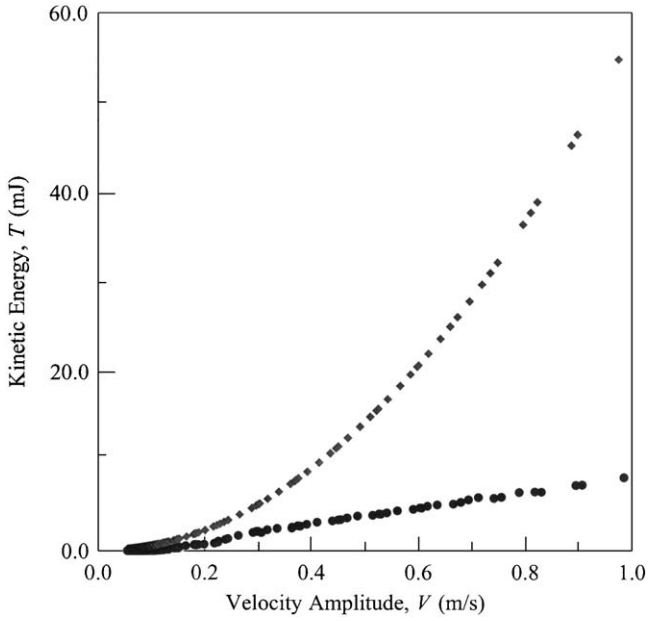

Fig. 4. Kinetic energy dissipated per cycle versus velocity amplitude. 1.2 mm lead spheres, $\mu = 0.1$ and $\Delta = 5.65$. ●, Energy dissipated; ◆, maximum kinetic energy.

significantly changes the mechanics of PID. This phenomenon is responsible for the peaks in $\Psi(\Gamma)$ in the vicinity of Γ_{cr} in Fig. 5 and in data reported in Ref. [12].

One of the most interesting results of the rather elementary model presented in Ref. [12] is the prediction that Ψ should depend on mass ratio by a factor of $\mu/(1+\mu)^2$. In order to test this particular prediction of the model, a mass normalized damping is now introduced as $\Psi_m = \Psi(1+\mu)^2/\mu$. Corresponding to Ψ presented in Fig. 5(a) for three values of μ, Ψ_m is plotted in Fig. 5(b). Within the experimental scatter, all three curves collapse into a single curve. Therefore, the dependence of Ψ on μ predicted in Ref. [12] is verified by the experiments.

4.2. The effect of the number of particles

We now raise the following question: All other parameters remaining the same (μ, Δ, and particle material), does the $\Psi(\Gamma)$ depend upon the total number of particles in the enclosure, N? Using glass spheres, and keeping $\mu = 0.02$ and $\Delta = 5.65$, N was varied by varying the diameter. Three different diameters were used: 0.5, 1.12, and 3 mm; the corresponding values of N are 11 000, 1035, and 50, respectively.

The results are presented in Fig. 6(a). For $\Gamma < \Gamma_{cr}$, Ψ is measurably the same for all three cases. For $\Gamma > \Gamma_{cr}$, Ψ is significantly smaller for $N = 50$. However, for $N = 1035$ and 11 000, Ψ is about the same. It is conjectured that the lower damping for $N = 50$ is due to a smaller number of inter-particle collisions, and that above some particular value of N, Ψ becomes independent of N. In order to further test this conjecture, the number of 3 mm diameter particles was doubled to 100 (μ

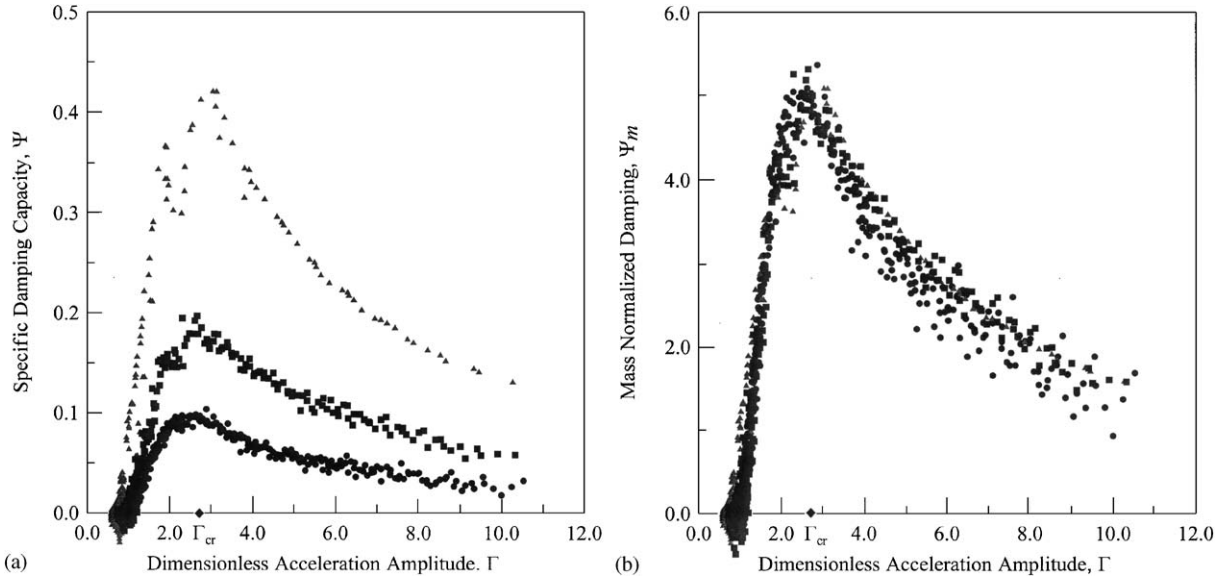

Fig. 5. (a) Specific damping capacity versus dimensionless acceleration amplitude, Γ. 1.2 mm lead spheres and $\Delta = 5.65$. (b) Mass normalized damping. ▲, $\mu = 0.1$; ■, $\mu = 0.04$; ●, $\mu = 0.02$.

is doubled to 0.04), and the measurement was repeated. The mass normalized PID obtained with 100, 1035, and 11 000 particles is compared in Fig. 6(b). The normalization is necessary because in going from Fig. 6(a) to 6(b), the aggregate mass of the 3-mm particles has doubled. Within the scatter of the data, Ψ_m is about the same for all three cases. In going from 50 to 100 particles the mass normalized damping increases significantly. It is concluded that at least for the values of N under consideration ($N \sim 50$), Ψ depends upon N.

4.3. The effect of particle material

Next, we examine the influence of particle material (lead, glass, or steel) on PID. Particles of nearly the same size were used: 1.12 mm glass spheres, 1.17 mm steel spheres, and 1.2 mm lead spheres. It was found that for 1.2 mm lead spheres, it took exactly 207 particles to cover the floor; we define this as one layer of particles. For glass, steel, and lead spheres one layer corresponds to a mass ratio (mass in grams) of 0.004 (0.41), 0.013 (1.33), and 0.02 (2.04), respectively. In order to make the comparison more meaningful, for each material, tests were conducted for one, two, and five layers of particles. For all cases, Δ was held constant at 5.65.

For one layer of steel and lead spheres, the mass normalized PID is compared in Fig. 7(a); for $\Gamma < \Gamma_{cr}$, Ψ for lead is noticeably greater than that for steel. (The results for one layer of glass spheres are not presented because the scatter in the data became very large after the raw data was divided by the small mass of the glass particles to produce the mass normalized data.) Clearly, for one layer the material makes a difference. PID for (exactly) two and five layers of lead, steel, and glass spheres is presented in Fig. 7(b) and (c), respectively. In going from one to five layers, the difference in $\Psi_m(\Gamma)$ decreases gradually; in Fig. 7(c), Ψ_m is the same for all three materials within

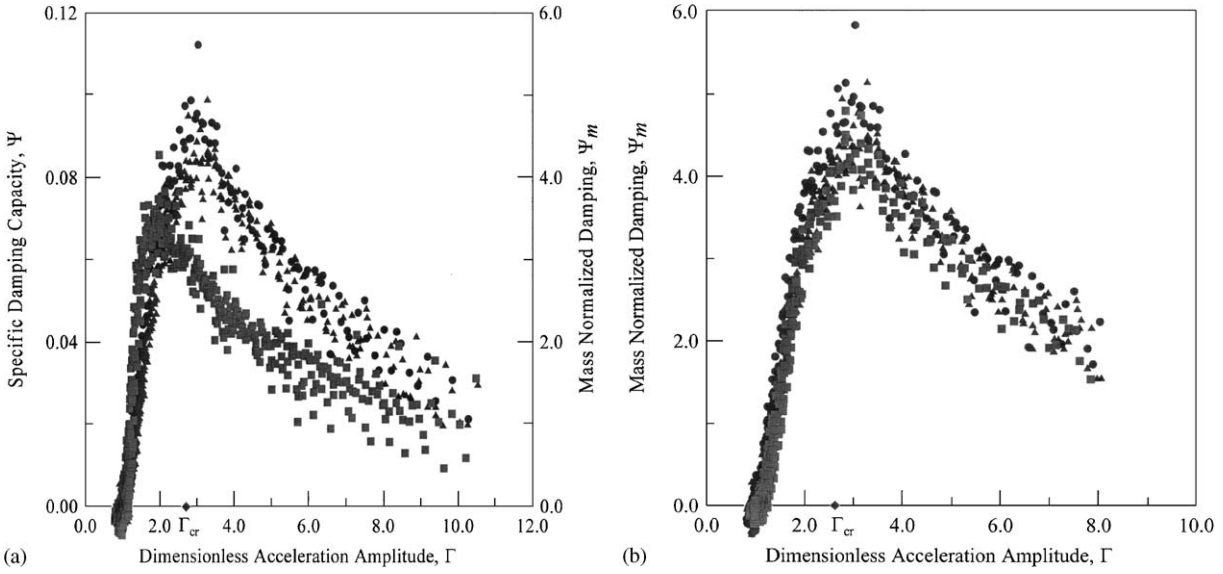

Fig. 6. (a) Comparison of damping for different number of particles for the same mass ratio. Glass spheres, $\mu = 0.02$, and $\Delta = 5.65$. ▲, 11 000 particles (0.5 mm diameter); ●, 1035 particles (1.12 mm diameter); ■, 50 particles (3 mm diameter). (b) Comparison of mass normalized damping for different number of particles. Glass spheres and $\Delta = 5.65$. ▲, 11 000 particles (0.5 mm diameter); ●, 1035 particles (1.12 mm diameter); ■, 100 particles (3 mm diameter).

the scatter of the data. Within the confines of the materials tested (steel, lead, and glass) it may be concluded that for a small number of particles, the material affects the PID; the effect of material seems to disappear as the number of particles increases.

In order to guard against drawing a conclusion based solely on data collected with one Δ, we now report the results of a series of tests with the following values of Δ: 1.13, 2.26, 3.36, 4.52, 5.25, or 7.91; μ was held constant at 0.06 throughout. Therefore it is unnecessary to mass normalize the damping. $\Psi(\Gamma)$ was measured for four different materials, namely, glass, steel, lead, and tungsten carbide. It was shown above that Ψ depends on N (albeit weakly) for small $N(N \sim 50)$. In order to eliminate N as an independent variable, N was chosen to be large $(620 < N < 7,500)$; see Table 1. The results are presented in Fig. 8(a)–(f). Once again, within the scatter in the data, the effect of material upon Ψ is rather weak. (It might be argued that Ψ for glass is slightly smaller than that for the other heavier materials.)

Fig. 8(f) deserves special attention because of a sharp dip at $\Gamma \approx 2.7 < \Gamma_{cr} = 3.18$. With reference to Fig. 9 of Ref. [12], imagine an enclosure without a ceiling. After being launched the particles fall under the action of gravity and hit the floor; the relative speed of impact, and hence the PID depends on Γ. The peak damping is achieved at $\Gamma = 2.49$ when the speed of the particle falling down is exactly equal to the speed of the beam going up (reminiscent of a head-on collision). If there had been no ceiling the damping in Fig. 8(f) would have continued to decrease with Γ until it would have become zero at $\Gamma = 4.38$ when, at the instant of impact, the velocity of the particle relative to that of the beam is zero. Therefore in Fig. 8(f), where there is a ceiling ($\Delta = 7.91$), the sudden reversal in the slope of $\Psi(\Gamma)$ curve at about $\Gamma = 2.7$ can only be attributed

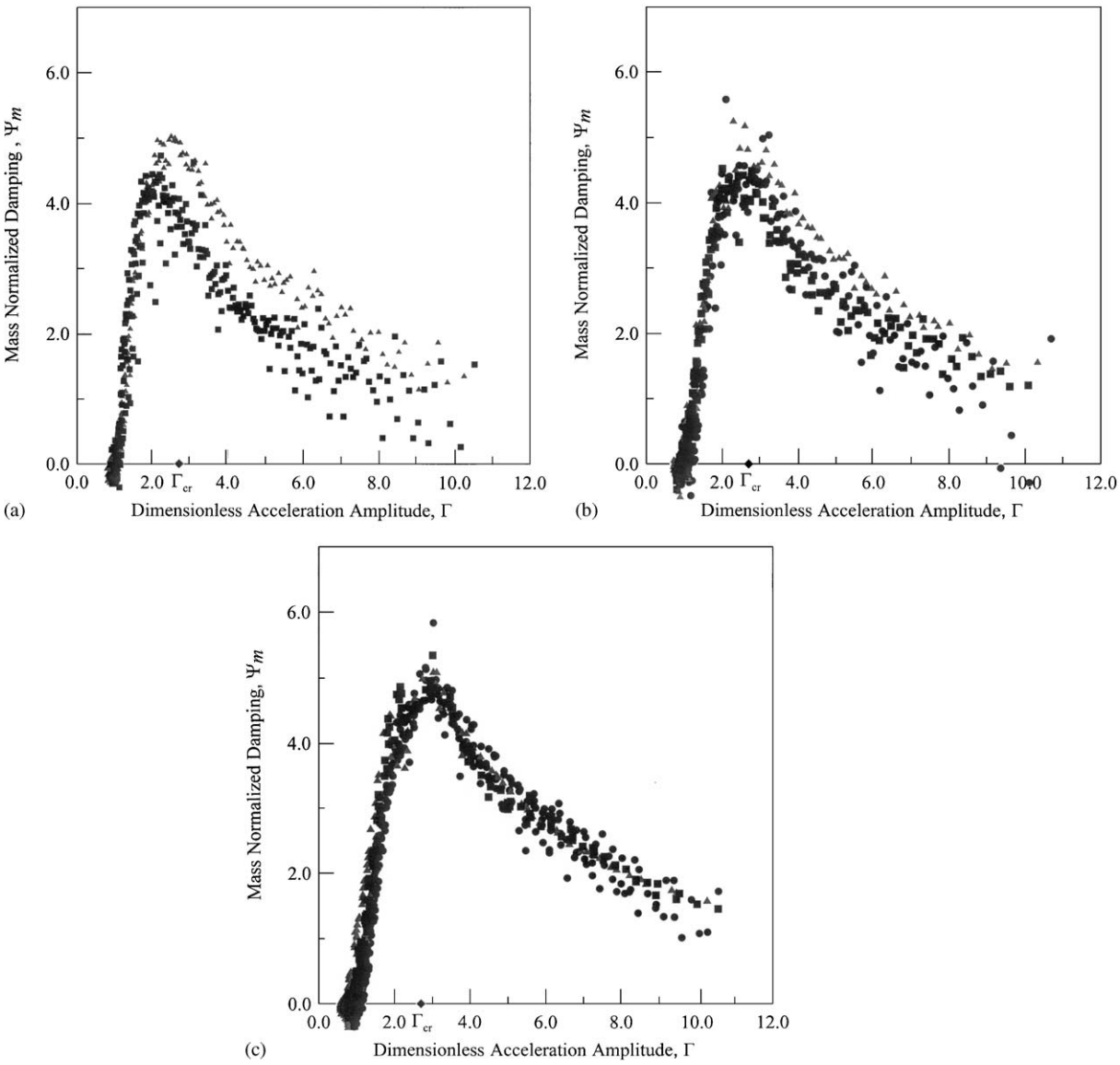

Fig. 7. Comparison of mass normalized damping for three different materials for the same size, shape, and number of particles, $\Delta = 5.65$. ▲, lead spheres; ●, glass spheres; ■, steel spheres. (a) One layer, 207 particles; (b) two layers, 414 particles; (c) five layers, 1035 particles.

to the particles hitting the ceiling. According to Ref. [12], if all the particles were flying like a single "particle", they would hit the ceiling at $\Gamma = \Gamma_{cr}$. The lack of coincidence of Γ suggests that the particles may not be flying like a single particle.

In order to bring the influence of Δ on Ψ into a sharper focus, a perspective view of the results presented in Figs. 8(a)–(f) is shown in Fig. 8(g); only the data for tungsten carbide is shown.

Table 1
Particles tested ($\mu = 0.06$)

Particle material	Diameter (mm)	Density (g/cm^3)	Approximate number of particles
Glass spheres	1.12	2.50	2800
Steel spheres	1.17	7.84	900
Lead spheres	1.20	11.3	620
Tungsten carbide Pellets	~0.50	13.0	7500

(Similar results were obtained with the other three materials, namely, glass, steel and lead. For brevity these are not included.) Evidently, when the clearance Δ is zero, Particle *Impact* Damping is zero. As Δ increases, at first Ψ increases, and then appears to level off at about $\Delta \approx 8$. Unfortunately, we did not collect data at higher values of Δ.

4.4. Dust-like particles

Much of the work presented so far was done with spherical particles. Next, we examine the damping due to very small irregularly shaped particles of lead, steel and sand; see Table 2 for material description. Note that N is very large: $13\,000 < N < 900\,000$. All tests were conducted with $\mu = 0.06$ and $\Delta = 5.25$. The results are plotted in Fig. 9, and they are quite unexpected. For the same values of μ and Δ, the data for larger particles of lead, glass, steel, and tungsten carbide has been presented in Fig. 8(e), and the reader is encouraged to compare the two figures.

First we consider $\Gamma < \Gamma_{cr}$ in Fig. 9. In all the measurements reported in this work and in Ref. [12], for the same μ and Δ, $\Psi(\Gamma)$ was found to be the same for all materials and particle sizes tested. This is the first observation when for $\Gamma < \Gamma_{cr}$, $\Psi(\Gamma)$ is different for the same μ and Δ. In all the previous data reported herein, at $\Gamma = \Gamma_{cr}$, $\Psi(\Gamma)$ is characterized by a peak. However, in Fig. 9, with the exception of lead, there is no peak at $\Gamma = \Gamma_{cr}$. Indeed, there is not even a discernible change in slope of $\Psi(\Gamma)$ at Γ_{cr}. One is forced to conjecture that for such a large number or such a small size of particles, the fundamental assumption of the model [12]—that all particles move together as a single "particle"—breaks down. The smoothness of the data around Γ_{cr} suggests that the particles are moving more like a "cloud of particles".

In Fig. 9, the data for *steel spheres* is reproduced from Fig. 8(e) as open squares. For the same μ, Δ, and material (steel), the damping for dust-like particles is significantly smaller than that for spheres. On the other hand, in the case of lead, the damping for the dust-like particles and the spheres is almost the same. Therefore, it cannot be concluded whether there is a difference in PID due to spherical and dust-like particles.

For values of Γ much larger than Γ_{cr}, the three curves appear to be converging. This may be explained as follows. At large Γ (recall that Γ is the acceleration amplitude in units of g) the time between the launch from the floor and the capture by the ceiling is very small; see Fig. 13(d) of Ref. [12]. One may conjecture that, during their flight from the floor to the ceiling, the particles do not have enough time to separate from each other. The singe-particle model of Ref. [12] would then predict a convergence of the three curves.

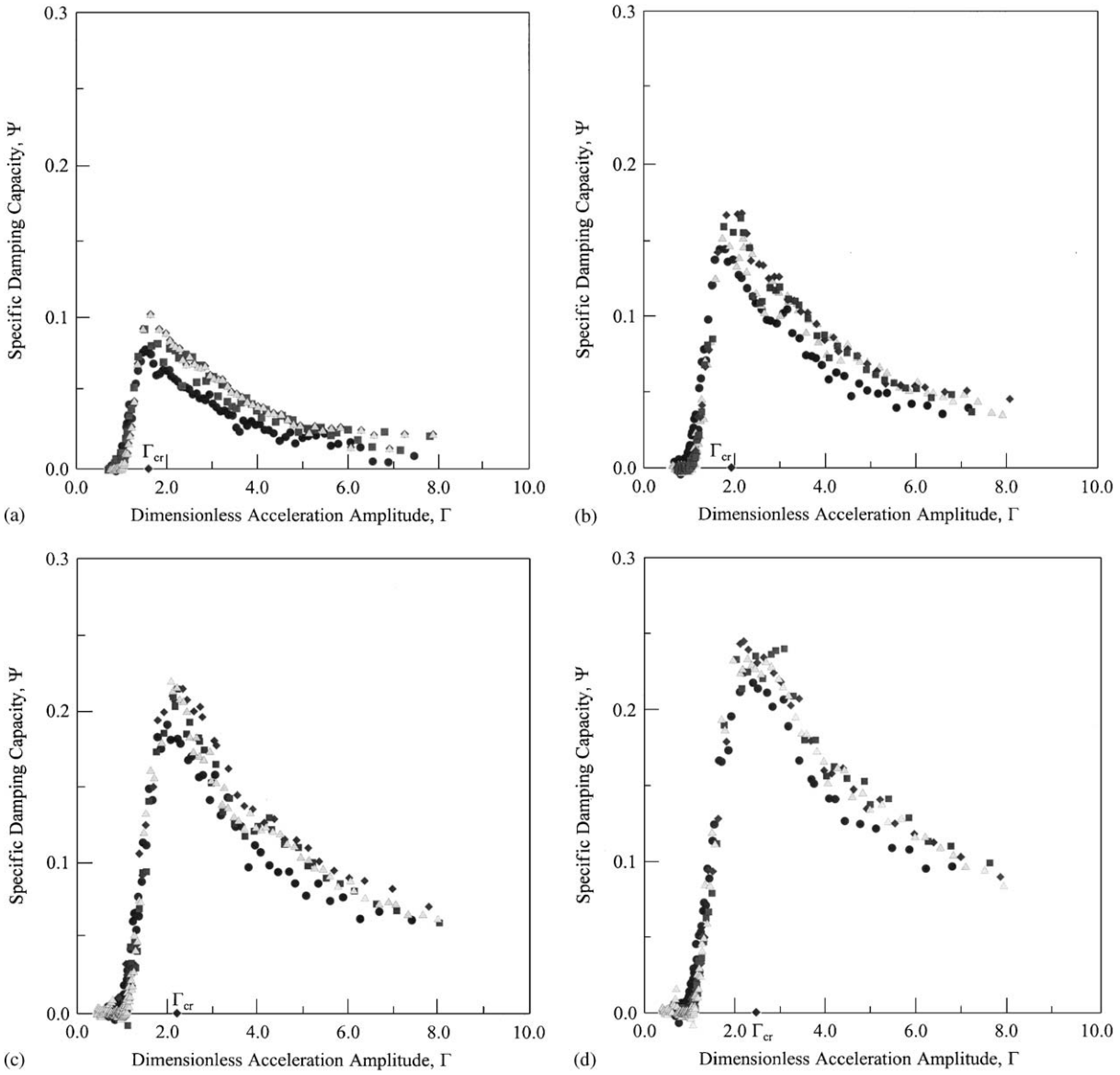

Fig. 8. Comparison of specific damping capacity for four different particle materials for the same mass ratio, $\mu = 0.06$; ●, glass spheres; ◆, steel spheres; ■, tungsten carbide; ▲, lead spheres. (a) $\Delta = 1.13$; (b) $\Delta = 2.26$; (c) $\Delta = 3.36$; (d) $\Delta = 4.52$; (e) $\Delta = 5.25$; (f) $\Delta = 7.91$; (g) the effect of Δ. Tungsten carbide:. ●, $\Delta = 1.13$, 3.36, and 5.25; ○, $\Delta = 2.26$, 4.52, and 7.91.

5. Conclusion

In Ref. [12] experimental results obtained with only one mass ratio (μ), one material (lead dust), one particle size (230 μm), and only three different values of clearance (Δ)

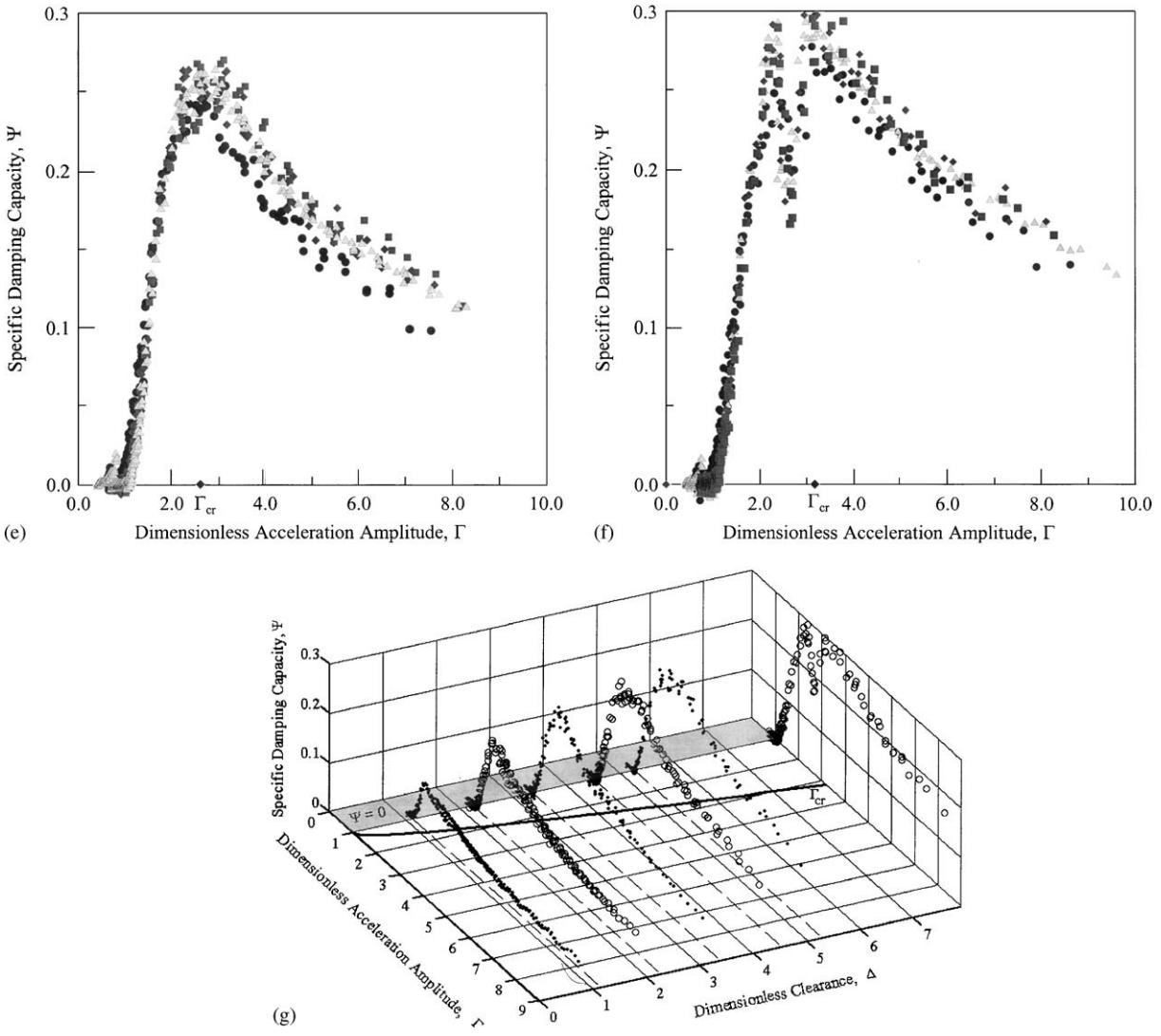

Fig. 8. (*Continued*)

were reported. The main objective of this work is to report a significant amount of additional particle impact damping (PID) data. Five materials have been tested: lead, steel, glass, tungsten carbide, and sand. The effect of mass ratio, number of particles, particle material, and shape of the particles on PID has been studied. The experimental results indicate that a more advanced model of PID must include the size and the number of particles as additional independent parameters, and remove the restriction of all particles moving as a single particle.

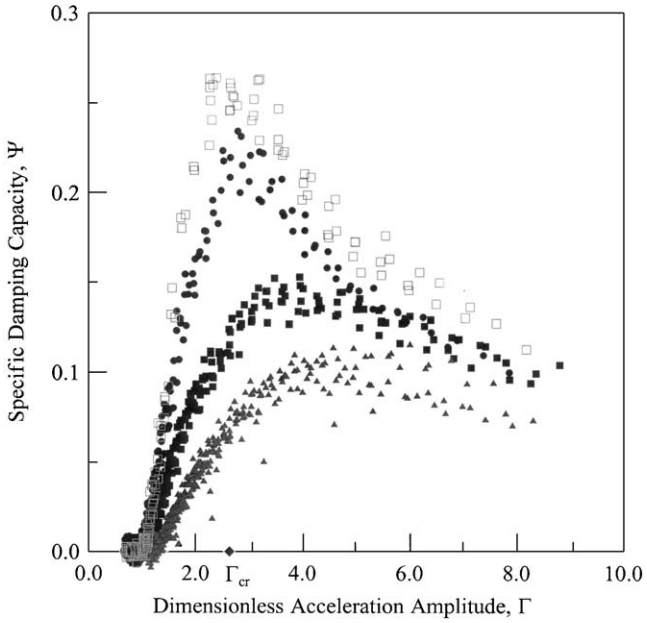

Fig. 9. Comparison of specific damping capacity for three different particle materials with dust-like particles, $\mu = 0.06$ and $\Delta = 5.25$: □, steel spheres; ●, lead dust; ■, steel dust; ▲, sand.

Table 2
Dust-like particles ($\mu = 0.06$)

Particle material	Average equivalent diameter (mm)	Density (g/cm^3)	Approximate number of particles
Sand	0.2	1.70	900 000
Steel dust	0.5	7.84	13 000
Lead dust	0.2	11.3	140 000

References

[1] C.M. Harris, C.E. Crede, *Shock and Vibration Handbook*, McGraw-Hill, New York, 1976, pp. 10–40.
[2] L.B. Erlikh, Vibration absorber with impact action and its use in machine tools, *The Engineer's Digest* 14 (1953) 31–32.
[3] D.I. Ryzhkov, Vibration damper for metal cutting, *The Engineer's Digest* 14 (1953) 246.
[4] C.N. Bapat, S. Sankar, Single unit impact damper in free and forced vibration, *Journal of Sound and Vibration* 99 (1985) 85–94.
[5] C. Saluena, T. Poschel, S.E. Esipov, Dissipative properties of vibrated granular materials, *Physical Review* 59 (1999) 4422–4425.
[6] Chen Tianning, Mao Kuanmin, Huang Xieqing, Michael Yu Wang, Dissipation mechanisms of non-obstructive particle damping using discrete element method, *Proceedings of SPIE International Symposium on Smart Structures and Materials,* Vol. 4331, Newport Beach, CA, March 2001, pp. 294–301.

[7] A. Papalou, S.F. Masri, Response of impact dampers with granular materials under random excitation, *Earthquake Engineering and Structural Dynamics* 25 (1996) 253–267.
[8] C. Cempel, G. Lotz, Efficiency of vibrational energy dissipation by moving shot, *Journal of Structural Engineering* 119 (1993) 2624–2652.
[9] N. Popplewell, S.E. Semergicil, Performance of the bean bag impact damper for a sinusoidal external force, *Journal of Sound and Vibration* 133 (1989) 193–233.
[10] H.V. Panossian, Nonobstructive particle damping (NOPD) performance under compaction forces, in: *Machinery Dynamics and Element Vibrations*, ASME DE-Vol. 36, 1991, pp. 17–20.
[11] H.V. Panossian, Structural damping enhancement via non-obstructive particle impact damping technique, *Journal of Vibration and Acoustics* 114 (1992) 101–115.
[12] R.D. Friend, V.K. Kinra, Particle impact damping, *Journal of Sound and Vibration* 233 (2000) 93–118.
[13] M. Saeki, Impact damping with granular materials in a horizontally vibrating system, *Journal of Sound and Vibration* 251 (2002) 153–161.